Journal of Photonic Materials and Technology
2021; 7(1): 1-7
http://www.sciencepublishinggroup.com/j/jpmt
doi: 10.11648/j.jmpt.20210701.11
ISSN: 2469-8423 (Print); ISSN: 2469-8431 (Online)

Influence of Post Annealing Rates on Porosity, Dispersion Energy and Associated Dielectric Energy Losses of TiO_2 Thin Films

Nelson Mugambi*, James Mbiyu Ngaruiya, Simon Waweru Mugo, Geoffrey Gitonga Riungu, Gitonga Mbae John

Department of Physics, Jomo Kenyatta University of Agriculture and Technology Nairobi, Kenya

Email address:

nelmug2013@gmail.com (N. Mugambi), ngaruyiajm@fsc.jkuat.ac.ke (J. M. Ngaruiya), wawerumugo@jkuat.ac.ke (S. W. Mugo), geoffreyriungu@gmail.com (G. G. Riungu), mbaejoni@gmail.com (G. M. John)

*Corresponding author

To cite this article:

Nelson Mugambi, James Mbiyu Ngaruiya, Simon Waweru Mugo, Geoffrey Gitonga Riungu, Gitonga Mbae John. Influence of Post Annealing Rates on Porosity, Dispersion Energy and Associated Dielectric Energy Losses of TiO_2 Thin Films. *Journal of Photonic Materials and Technology*. Vol. 7, No. 1, 2021, pp. 1-7. doi: 10.11648/j.jmpt.20210701.11

Received: December 20, 2020; **Accepted**: January 18, 2021; **Published**: January 25, 2020

Abstract: With scientific and technological advances, Titanium dioxide (TiO_2) has attracted great research interest in the field of Dye Sensitized Solar cells (DSSC) with an aim to improve its efficiency. In this study, transparent semiconducting titanium dioxide thin films were deposited on glass substrate coated with fluorine tin IV oxide (SnO_2: F) film by sol gel technique. The films were then annealed in air up to 450°C at different annealing rates. Optical reflectance was measured using UV-Vis-NIR spectrophotometer and optical parameters such as refractive index, extinction coefficient and dielectric constants were modelled using SCOUT software. Average refractive indices in the visible region ranged between 1.95 and 1.56. Porosity for as deposited, 1 step, 2°C/min and1°C/min were found to be 48%, 73%, 61% and 53% respectively. Refractive index dispersion was investigated using Wemple – Di-Domenico single oscillator model. Dispersion energy of annealed films increased from 5.90 eV to 11.30 eV. Surface and volume energy loss were computed from dielectric constants and correlated with porosity and dispersion energy as function of the heat treatment. Optical parameters were found to highly depend on the annealing the thin films. Annealing rate influenced a decrease in porosity and an increase in dispersion energy due to film densification and pore filling as the crystallinity is improved by heat treatment.

Keywords: TiO_2, Surface Energy Loss, Thin Film, Volume Energy Loss, Porosity, Dispersion Energy

1. Introduction

Renewable energy sources such as solar energy provide a more environmental friendly source of power. However, photovoltaics use is still limited due to high cost of production and low energy conversion efficiency [1]. The low energy conversion efficiency of devices such as dye sensitized cells (DSSC's) can be improved through nanotechnology [2]. TiO_2 nanoparticles (NPs) have been considered for dye sensitized cells due to high photocatalytic and sonocatalytic efficiency, low toxicity, excellent biocompatibility, low cost and high chemical stability [3, 4]. The anatase phase is highly attractive in titanium oxides coatings due to its low extinction coefficient and high refractive index [5]. It is found that TiO_2 films with an anatase phase can achieve a higher efficiency for a DSSC than TiO_2 films with a rutile one [6, 7]. TiO_2 films of high homogeneity and thickness over a large area are available at low annealing temperature through Sol-gel technique [8].

TiO_2 can exist as an amorphous layer and also in three crystalline phases: brookite (orthorombic) anatase (tetragonal) and rutile (tetragonal). Only rutile phase is thermodynamically stable at high temperatures [9]. Annealing of TiO_2 films alters crystallinity, electrical resistivity, surface porosity as well as morphology [9]. Optical characterization of TiO_2 thin films by UV-visible spectrophotometry has been done [10] and Scout software used in analysis of optical measurements such as transmittance and reflectance [11]. The structural properties of

the mesoporous TiO_2 films, such as particle size [12] and porosity [12, 13] have a significant influence on the performance of DSSC's. Highly porous TiO_2 films promote increased light absorption and a higher current density [14, 15]. Increasing the surface area and porosity of TiO_2 films decreases the contact barrier between the TiO_2 and subsequent interfaces, which promote the transport of carriers in the DSSCs [16]. The dispersion parameters of TiO_2 films obeys the single oscillator model and the dispersion parameters decreases with increasing annealing temperature [17]. TiO_2 films were deposited by so-gel doctor blade technique since it is a simple, low cost technique, and offers good uniformity. The effect of annealing rates on the dispersion energy, porosity and surface to volume energy loss were investigated.

2. Experimental Procedure

Nanocrystalline TiO_2 (T/SP, 18% wt, 15-20 nm, sourced from Solaronix, Switzerland) was coated on FTO (SnO_2: F) 7 Ω/sq, (Xinyan Technology Co. Limited, China) glass substrates using sol-gel doctor-blading technique. Freshly prepared films were annealed at different rates using muffle furnace. The samples were annealed at 1 step 2°C /min and 1°C/min annealing rates. The temperature was increased at the stated rates up to 450°C followed by sintering for 30 minutes.

The optical reflectance was measured using double beam UV-Visible spectrophotometer (Shimadzu UV probe 1800, Japan) in the wavelength range of 200-1100 nm. The optical constants such as refractive index (n), extinction coefficient (k) and dielectric constants ($\varepsilon_1, \varepsilon_2$), were obtained using SCOUT software. The dielectric tangent loss and the dielectric energy loss of these films were also studied on different annealing rates. Determination of the dispersion parameters of the samples such as the high-frequency dielectric constant ε_∞, the oscillator energy E_o and the dispersion energy E_d was achieved by application of Wemple-Di Domenico single oscillator model.

3. Results and Discussion

3.1. Reflectance

Figure 1 shows reflectance versus wavelength spectra for annealed TiO_2 films. Reflectance decreases within the visible region. Room temperature deposited TiO_2 thin film shown only about 20% reflectance, which can be useful for antireflection coating. The film with the lowest annealing rate (1°C/min) has the highest reflectance while 1 step (highest annealing rate) film has lowest reflectance.

We attribute the increase in reflectance as observed in figure 1 to improved crystallinity due to decrease in lattice imperfections and enhanced homogeneity due to annealing. Ayieko *et al* reported an increase in reflectance at higher annealing temperatures due to decrease in crystallite sizes hence resulting in surface area of particles to scatter light [18]. The higher reflectance is attributed to the improvement in crystallinity and a rise in thermal conductivity [19].

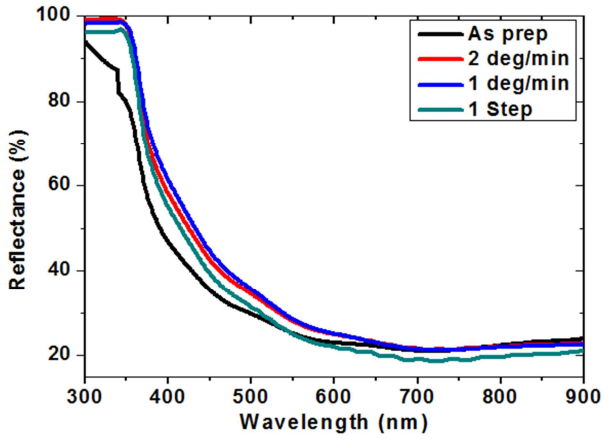

Figure 1. *A graph Reflectance versus Wavelength.*

3.2. Refractive Index

Analysis of the reflectance data was done using Scout software. The real part $\varepsilon_1$and imaginary part ε_2 of dielectric constant as in equation (1) and (2) were obtained;

$$\varepsilon_1 = n^2 - k^2 \quad (1)$$

$$\varepsilon_2 = 2nk \quad (2)$$

Where n is the refractive index and k is the extinction coefficient. The refractive indices of the samples were determined from the relation in equation (3).

$$n = \left[\frac{1+R}{1-R}\right] + \sqrt{\frac{4R}{(1-R)^2} - k^2} \quad (3)$$

Where R is the reflectance and k is the extinction coefficient. Figure 2 shows variation of refractive index of annealed TiO_2 films verses wavelength, λ. The refractive index spectra were found to decrease exhibiting high variation towards the low photon energy indicating normal dispersion behavior. The decrease of the refractive index as shown in figure 2 indicates that the material is less optically dense.

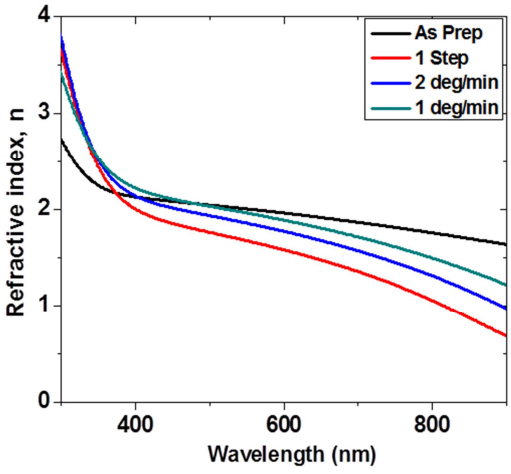

Figure 2. *A graph of refractive index versus wavelength.*

Figure 3 shows average refractive indices within the visible region as a function of annealing rates.

The average refractive indices in the visible region for as prepared, 1 step, 2°C/min and 1°C/min were found to be 1.95, 1.56, 1.75, and 1.87 as shown in figure 3 respectively. A rise in refractive index values is observed with decreasing annealing rates. The decrease in refractive index was associated with the resonance effect. This effect occurs between electronic polarization and incident light photons on the sample due to equality between the incident photon and plasma frequency [20]. This increase in refractive index with annealing is dependable with the fact that there occurs enhancement of crystallinity and higher packing density as the annealing rates is lowered [20].

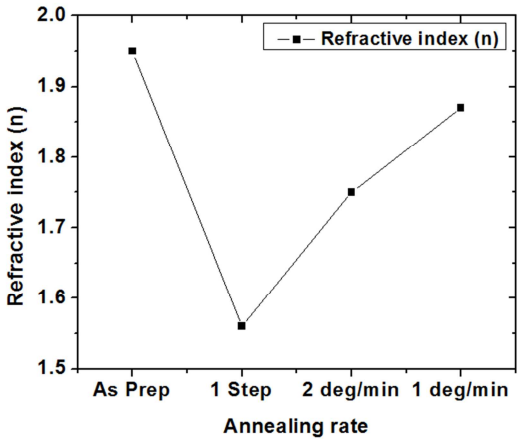

Figure 3. A graph of refractive index versus annealing rate.

3.3. Porosity and Relative Density of Annealed TiO_2 films

The porosity and relative density of the film were calculated using equation 4 [21] and 5 [22];

$$Porosity = (1 - \frac{n^2-1}{n_0^2-1}) \times 100\% \quad (4)$$

$$Relative\ density = \frac{n^2-1}{n_0^2-1} \times 100\% \quad (5)$$

Where n is the refractive index of the films and $n_0 = 2.52$ the refractive index of anatase TiO_2 [23]. Figure 4 shows variation of relative density and porosity with annealing rates.

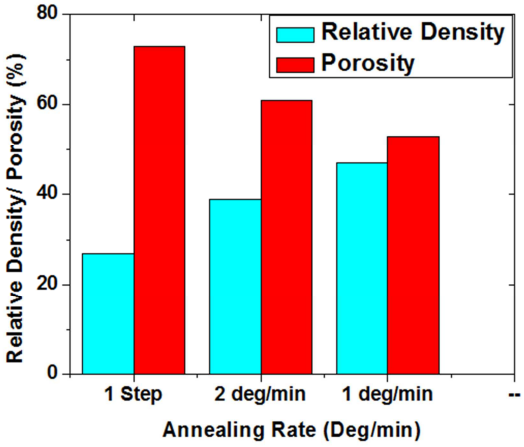

Figure 4. Variation of relative density and porosity with decreasing annealing rates.

The porosity of the films decreases while the relative density increases with lowering of annealing rate. 1 step film has the highest porosity of 73% and the least relative density of 27%. Hasan *et al*, [24] analyzed XRD patterns of as-deposited and annealed TiO_2 films at different temperatures. Crystallization was found to increase to some extent in the annealed films. Increase in annealing temperature was found to decrease porosity ratio of the films. Decrease in porosity as shown in figure 4 is attributed to film pore filling and film densification. The increase in relative density due to annealing rates, indicate that the quality of the film crystallization improves gradually. The porosity has been correlated with dispersion energy discussed in the following section.

3.4. Refractive Index Dispersion Parameters

The functional relation for the dispersion of refractive index was done using the single oscillator model suggested by Wemple - DiDomenico model given by equation 6 [25, 26]

$$(n^2 - 1)^{-1} = \frac{E_0}{E_d} - \frac{1}{E_0 E_d}(h\nu)^2 \quad (6)$$

Where E_0 is the single oscillator energy, and E_d is the dispersion energy.

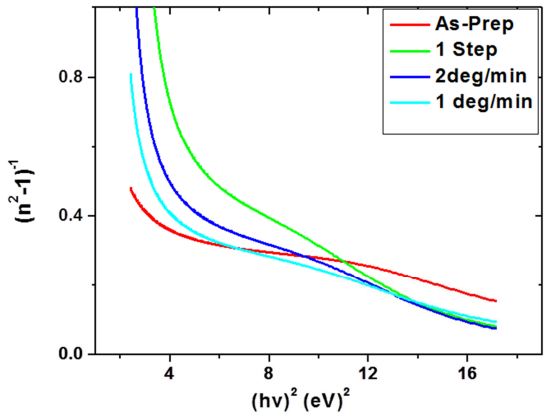

Figure 5. Plot of $(n^2-1)^{-1}$ versus $(h\nu)^2$ of annealed TiO_2 coatings.

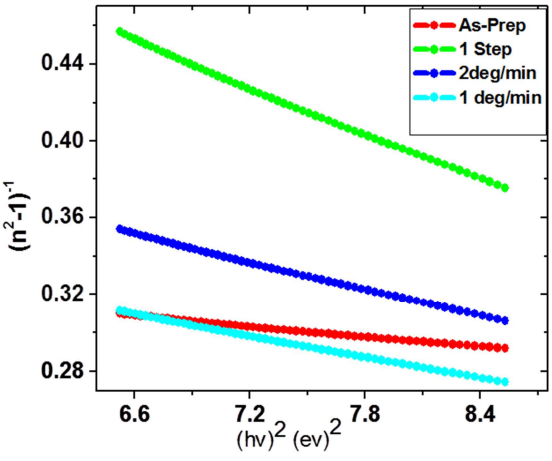

Figure 6. Linear fit of $(n^2-1)^{-1}$ versus $(h\nu)^2$ of annealed TiO_2 films.

Table 1. *Optical parameters and dispersions of TiO_2 thin films at various annealing rates.*

Samples	Refractive index, n	Relative density (%)	Porosity (%)	E_d	E_0	M_{-1}	M_{-3}	$f=E_d E_0$
As-Prep	1.95	52	48	17.46	6.41	2.72	0.42	111.9
1 Step	1.56	27	73	5.90	4.23	1.39	0.33	24.96
2°C/min	1.75	39	61	9.15	4.64	1.97	0.42	42.46
1°C/min	1.87	47	53	11.30	4.85	2.33	0.48	54.81

Figure 5 shows spectra of $(n^2-1)^{-1}$ against $(hv)^2$ for TiO_2 films before and after annealing. The values of $(n^2-1)^{-1}$ decreases as the photon energy increases for all the films due to the lattice absorption [26]. The oscillator energy, E_o and dispersion energy, E_d were obtained by fitting a straight line to the spectra of $(n^2-1)^{-1}$ versus $(hv)^2$ from 6.6 to 8.4 $(eV)^2$ as shown in figure 6. The $(n^2-1)^{-1}$ intercept of the linear fit gives E_o/E_d and the slope gives $(E_oE_d)^{-1}$. The values of oscillator energy E_o and dispersion energy E_d for film annealed at 1°C/min were 4.85eV and 11.30eV respectively. Wemple - DiDomenico defines the oscillator strength, f, for a single oscillator model given as $f=E_oE_d$. The results of oscillator strength are included in table 1. E_o and E_d are dependent on the moment of the optical transitions M_{-1} and M_{-3} defined by $E_o^2=M_{-1}/M_{-3}$ and $E_d^2=M_{-1}^3/M_{-3}$ and the calculated values listed in table 1. M_{-1} and M_{-3} decreased with increase in annealing rates. From earlier work, increase in E_0 and E_d as a result of increase in annealing temperature has been attributed to influence of lattice absorption and increase in scattering centers [26]. The porosity is correlated with surface energy/volume energy loss discussed in the following section.

3.5. Dielectric Characterizations

Real part (ϵ_1) and imaginary part (ϵ_2) of the dielectric function were obtained using scout software as in equation 1 and 2. The ϵ_1 and ϵ_2 shows the amount of energy stored in dielectrics as polarization and loss energy respectively. The power loss factor (tan δ) associated with the electric behavior of the film is described by equation 7;

$$\tan\delta = \frac{\varepsilon_2}{\epsilon_1} \tag{7}$$

Inelastic scattering of electrons in solid film due to energy loss functions also known as volume energy function and surface energy loss function were calculated as in equation 8 and 9;

$$V_{el} = \frac{\epsilon_2}{\epsilon_1^2+\epsilon_2^2} \tag{8}$$

$$S_{el} = \frac{\epsilon_2}{(1+\epsilon_1)^2+\epsilon_2^2} \tag{9}$$

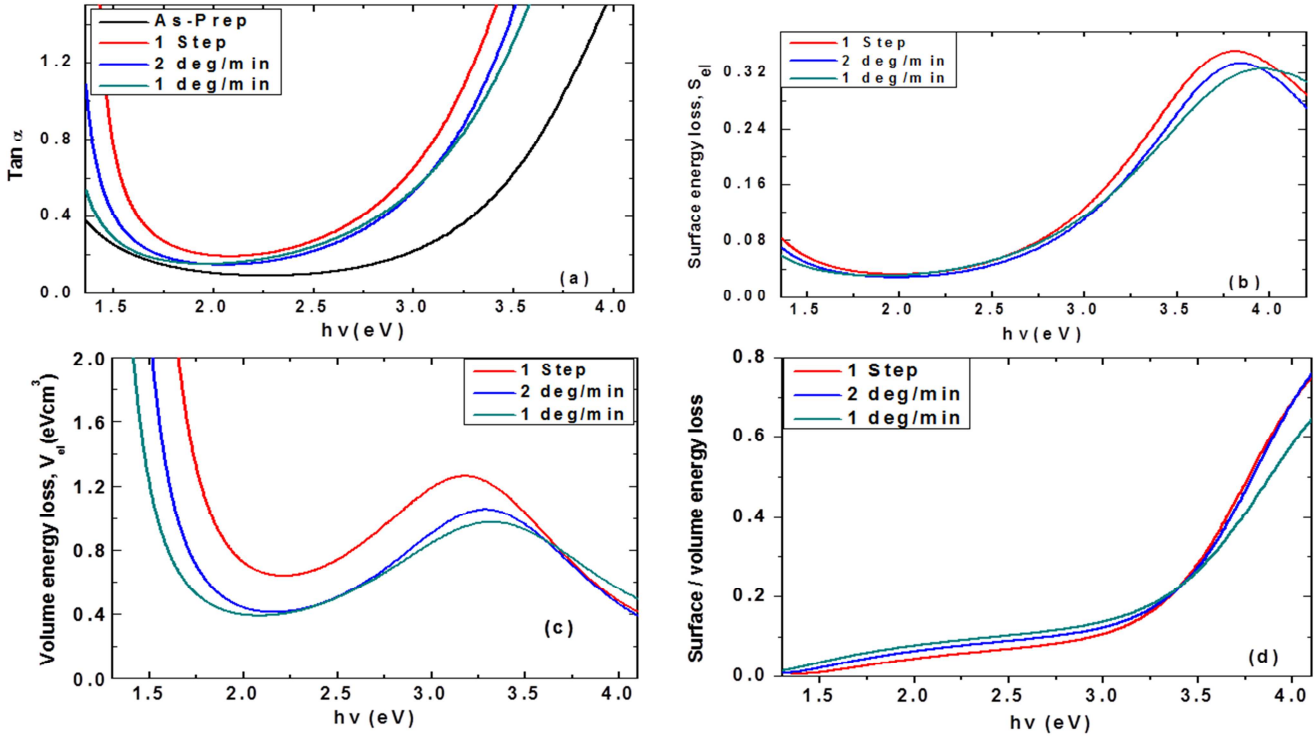

Figure 7. *(a). Loss tangent, (b) Surface energy loss, (c) volume energy loss, and (d) Surface / Volume enrgy loss as a function of photon energy.*

Tan δ describes the loss factor, which measures the loss rate of power in an oscillatory dissipative system. Figure 7 (a) shows a variation of tan δ versus photon energy for as prepared and annealed TiO_2 films. It is clearly seen than the values of tan δ decreases at lower photon energy (up to 2.0 eV) and thereafter increases gradually. In lower photo energy

(or low frequency) region (up to 2.0 eV) the tan δ value of the films decreases gradually with the decrease of annealing rates. However, for photon energy > 2.5 eV (or high frequency range), the loss tangent increases significantly with phonon energy. Since tan δ is less than 1 for all samples, then the energy loss of the films is relatively low. This suggests that the annealed films possess good optical qualities due to lower energy losses and lower scattering of the incident radiation [27]. The surface energy loss, S_{el} and volume energy loss, V_{el} functions of the TiO_2 films before and after annealing at different rates are shown in figure 7 (b) and (c) respectively. The surface energy loss peaks appears at approximately 4 eV for 1 step, 2°C/min and 1°C/min and their energy values were 0.351, 0.333 and 0.326 $eVcm^2$. The loss is relatively low at other photon energies. The peaks for volume energy loss appear at 3.22eV. They are relatively higher compared to surface energy loss.

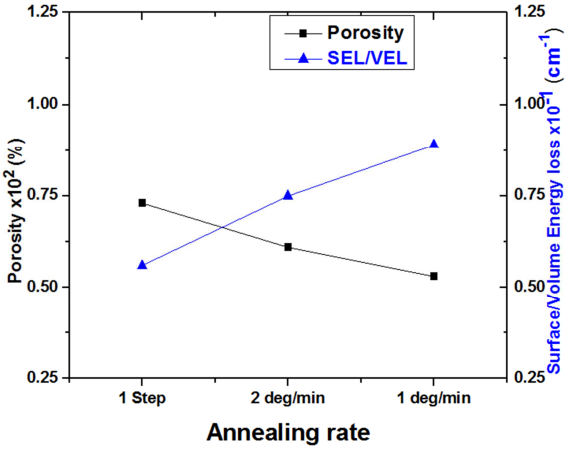

Figure 8. *Correlation of Porosity and surface/volume energy loss of annealed TiO_2 films.*

Volume energy function is much greater compared to surface energy functions (V_{el} and S_{el}) for all the incident photon energies at all annealing conditions. From earlier report, loss of energy of a free charge passing through the surface of film is less than when travelling through the volume [27-29]. Energy loss is experienced when a fast moving electron pass through a medium due to the excitation of plasma oscillations of conducting electron [29]. For all the annealed films, the energy losses for 1°C/min are the lowest. This is due to regular grain boundaries, which offer minimal energy dissipation. Figure 7 (d) shows the surface energy loss/volume energy loss against the photon energy. The ratio of surface to volume energy loss increases with decreasing annealing rate up to 3.5eV. At low photon energies, S_{el} is insensitive to surface structure and it does not describe the inelastic scattering with finite momentum transferred at the surface [30]. Therefore, the decrease in annealing rate increases the electron transition of the films. This is due to major contribution of virtual electronic transition in the TiO_2 thin films which leads to a significant change in the optical parameters [31]. In the inter-band region there is an appreciable modification of the refractive index as shown in figure 2. The ratio of surface to volume energy loss has been correlated with porosity and dispersion energy as shown in figure 8. The film annealed at the highest rate (1 Step) has the highest porosity. However, porosity is found to decrease with annealing rate.

We attribute the decrease in porosity to film pore filling and film densification due to crystal enhancement of the films with annealing. Surface/volume energy losses increases with decrease in annealing rate as shown in figure 7. It has been reported that annealing temperature and annealing time has an effect on surface quality porosity and aggregate of the films [32]. The surface of TiO_2 showed clustered particles through SEM and the shrinkage rate increased as result of heat treatment [32, 33]. Values for S_{el} and V_{el} are associated with the ionicity of ionic or covalent materials and crystalline structure [26]. The single oscillator model can essentially be applied in determination of the structural properties of these films in addition to the optical characterization [34]. From literature, the degree of electron transition decreases with improvement in crystallinity of the film hence increasing the free electron density. The frequency dependence of the complex electronic dielectric constant inferred the fundamental electron excitation spectrum of the thin film [35, 36]. Therefore, we associate the increase in S_{el}/V_{el} to improvement of crystalline quality of the TiO_2 films. The surface to volume ratio has the same trend with dispersion energy.

4. Conclusions

TiO_2 thin films (As deposited) deposited on fluorine tin oxide were prepared by sol gel doctor blade followed by annealing at 1 step, 2°C /min and 1°C /min annealing rates. Refractive index was used to study the optical parameters of the films samples in the spectra range 300 nm to 900 nm. Wemple – DiDomenico single ascillator model was used to determine the optical parameters. For all films, absorption coefficients were in the order of $10^5 cm^{-1}$. Computed dispersion, E_d and single oscillator energy Eo using W-D model was found to be in the range 5.90 – 17.46 eV and 4.23 – 6.41 eV respectively. The energy loss (Tan δ) was relatively low with the 1°C/min being the lowest. The volume and surface energy loss followed the same trend as the loss tangent data. Surface energy loss of the films was lower compared to the volume energy loss.

References

[1] Elano S., Guillermo R. and Javier G. (2009). "Nanotechnology for Sustainable Energy," *Renewable and Sustainable Energy Revolution paper*. 2337-2384.

[2] Du, J., Lai, X. Y., Halpert, E. J., Yang, Y. and Wang, D. (2011) "Formation of efficient dye sensitized solar cells by introducing an interfacial layer of hierarchically ordered macro-mesoporous TiO_2 film", *Science China Chemistry*, 54: 930.

[3] Khalid, N. S., Fazli, F. I., Abd H. N., Napi, M. L., Soon, C. and Ahmad, M. K. (2016). "Biocompatibility of TiO_2 nanorods and nanoparticles on HeLa cells" *Journal of Nanoscience and Nanotechnology*, 45: 1675-1678.

[4] Sung Y. M. and Kim H. J. (2007). "Sputter deposition and surface treatment of TiO2 films for dye-sensitized solar cells using reactive RF plasma," Thin Solid Films, 515: 4996-4999.

[5] Wang W. H., and Chao, S. (1998). "Annealing effect on ion-beam-sputtered titanium dioxide film," *Optics letters*, 23 (18), 1417-1419.

[6] Barbe C. J., Arendse F., Comte P., Jirousek M., Lenzmann F., Shklover V. and Gratzel M. (1997). "Nanocrystalline Titanium Oxide Electrodes for Photovoltaic Applications," *Journal of the American Ceramic Society*, 80 (12) 3157-3171.

[7] Park N. G., Van de Lagemaat J., and Frank A. J. (2000). "Comparison of Dye-Sensitized Rutile- and Anatase-Based TiO_2 Solar Cells," *National Renewable Energy Laboratory*, 104: 8989.

[8] Wang Y-H., Rahman K. H., Wu C-C., Chen K-C. (2020). "A Review on the Pathways of the Improved Structural Characteristics and Photocatalytic Performance of Titanium Dioxide (TiO_2) Thin Films Fabricated by the Magnetron-Sputtering Technique". *Catalysts*, 10 (6): 598.

[9] Hasan, M. M., Haseeb, A. S. M. A., Saidur, R., Masjuki, H. H. and Hamdi. M. (2009) "Synthesis and Annealing of Nanostructured TiO_2 Films by Radio-Frequency Magnetron Sputtering", Journal of Applied Sciences, 9: 2815-2821.

[10] Sta I, Jlassi M, Hajji M, Boujmil M. F, and Jerbi R. (2014), "Structural and optical properties of TiO_2 thin films prepared by spin coating', Journal of Sol-Gel Science and Technology 72: 421-427.

[11] Theiss, W. (2000). Scout thin films analysis software handbook, edited by Theiss M (Hand and Software Aachen German) www.mtheiss.com.

[12] Yang Y., Ri K. and Mei A. (2015). "The size effect of TiO_2 nanoparticles on a printable mesoscopic perovskite solar cell," *Journal of Materials Chemistry,* 3: 9103–9107.

[13] Kim H. S. and Park N. G., (2014). "Parameters affecting I–V hysteresis of $CH_3NH_3PbI_3$ perovskite solar cells: effects of perovskite crystal size and mesoporous TiO_2 layer," *Journal of Physical Chemistry Letters*, 5: 2927–2934.

[14] Liu H., Huang Z., Wei S., Zheng L., Xiao L., and Gong Q. (2016). "Nano-structured electron transporting materials for perovskite solar cells," *Nanoscale,* 8 (12) 6209–6221.

[15] Lu H., Deng K., Yan N. (2016). "Efficient perovskite solar cells based on novel three-dimensional TiO_2 network architectures," *Science Bulletin*, 61 (10) 778–786.

[16] Kim Y. J., Lee Y. H. and Lee M. H. (2008). "Formation of efficient dye-sensitized solar cells by introducing an interfacial layer of long-range ordered mesoporous TiO_2 thin film," *Langmuir,* 24 (22): 13225–13230.

[17] Chiad, Sami O., Saad B., Nabeel H., Nadir. (2014). "Electronic Transitions and Dispersion Parameters of Annealed TiO_2 Films Prepared by Vacuum Evaporation Technique," *Materials Focus,* 3: (10) 1134.

[18] Ayieko C. O., Musembi R. J., Waita S. M., Aduda B. O. and Jain P. K. (2003) "Structural and Optical Characterization of Nitrogen-doped TiO_2 Thin Films Deposited by Spray Pyrolysis on Fluorine Doped Tin Oxide (FTO) Coated Glass Slides," *International Journal of Energy Engineering*, 2 (3): 67-72.

[19] Xinmi H., Xiao X., Zhang, Z., Yang, J., and Zhang J. (2017). "Influence of surface topography, crystallinity, and thermal conductivity on reflectance and color of metallic-effect high-density polyethylene parts filled with aluminum pigments," *Polymer Engineering & Science*. 58. 10.1002/pen.24593.

[20] Hassanien A. S. and Akl A. A. (2018). "Optical characteristics of iron oxide thin films prepared by spray pyrolysis technique at different substrate temperatures," *Applied Physics A*. 124. 10.1007/s00339-018-2180-6.

[21] Liu X., Jin Z. and Bu S. (2005). "Influences of Solvent on Properties of TiO_2 Porous Films Prepared by a Sol-Gel Method from the System Containing PEG," *Journal of Sol-Gel Science and Technology,* 36 (1), 103–111.

[22] Ohyama M., Kozuka H. and Yoko T. (1997) "Sol-gel preparation of ZnO films with extremely preferred orientation along (002) plane from zinc acetate solution," *Thin Solid Films,* 306: 78-85.

[23] Kingery W. D., Bowen H. K. and Uhlmann D. R. (1976) Introduction to Ceramics, *Wiley, New York*.

[24] Hasan, M. M., Haseeb, A. S. M. A., Saidur, R., Masjuki, H. H., & Hamdi, M. (2010). Influence of substrate and annealing temperatures on optical properties of RF-sputtered TiO_2 thin films. *Optical Materials*, 32 (6): 690-695.

[25] Wemple S. H. and Di Domenico M. (1969) "Oxygen-Octahedra Ferroelectrics. II. Electro-optical and Nonlinear-Optical Device Applications," *Journal of Applied Physics*, 40: 735.

[26] Wemple S. H. and DiDomenico M. (1971) "Behavior of the Electronic Dielectric Constant in Covalent and Ionic Materials," *Physical Review B,* 3: 1338–51.

[27] Yang C., Fan H., Xi Y., Chen J. and Li Z. (2008) "Effects of depositing temperatures on structure and optical properties of TiO_2 film deposited by ion beam assisted electron beam evaporation" *Applied Surface Science*, 254: 2685-2689.

[28] Yakuphanoglu F., Cukurovali A. and Yilmaz I., Phys. B, (2004), Single-Oscillator Model and Determination of Optical Constants of Some Optical Thin Film Materials, *Physica B Condensed Matter,* 353: 210–216.

[29] Sarkar S., Das N. S. and Chattopadhyay K. K. (2014), Electro-active phase formation in PVDF–$BiVO_4$ flexible nanocomposite films for high energy density storage application, *RSC Advances*, 33: 58–66.

[30] El-Nhass, M. M., Soliman, H. S. and El-Denglawey, A. (2016), "Absorption edge shift, Optical conductivity and energy loss function of nano thermal-evaporated N-type anatase TiO_2 films," *Aplied physics A* 122: 775.

[31] Ali, A. I., Son, J. Y., Ammar, A. H., Abdel Moez, A. and Kim Y. S. (2013) "Optical and dielectric results of $Y_{0.225}Sr_{0.775}CoO_{3\pm\delta}$ thin films studied by spectroscopic ellipsometry technique", *Results in Physics*, 3: 167-172.

[32] Al-Jufairi, N. (2006), "Structure and Surface Properties of Anatase TiO_2 Thin Film by Sol-Gel Technique," *Materials Science Forum*, 517: 165–172.

[33] Al-jufairi J. N. (2012). "Electric properties and surface structure of TiO_2 for solar cells", *Energy*, 39: 6.

[34] Yakuphanoglu K. F., Cukurovali A. and Yilmaz I. (2004), "Single-Oscillator Model and Determination of Optical Constants of Some Optical Thin Film Materials," *Physica B Condensed Matter*, 353: 210–216.

[35] Fournier L. C., Bamiduro O., Mustafa H., Mundle R., Konda R. B., Williams F. and Pradhan A. K. (2008), "Effects of substrate temperature on the optical and electrical properties of Al: ZnO films" *Semiconductor Science and Technology*, 23: 085019.

[36] Zhiwen Q., Haibo G., Xiaopeng Y., Zichao Z., Jun H., Bingqiang C., Daisuke N. and Tatsuo O. (2015). "Phosphorus Concentration Dependent Microstructure and Optical Property of ZnO Nanowires Grown by High-Pressure Pulsed Laser Deposition," *The Journal of Physical Chemistry, C*. 119 (8), 4371-4378.